Published in final edited form as:
Exp Toxicol Pathol. 2014 March ; 66(0): 129–138. doi:10.1016/j.etp.2013.11.005.

Histopathological and immunohistochemical evaluation of nitrogen mustard-induced cutaneous effects in SKH-1 hairless and C57BL/6 mice

Anil K. Jain[a,**], **Neera Tewari-Singh**[a,**], **Swetha Inturi**[a], **David J. Orlicky**[b], **Carl W. White**[c], and **Rajesh Agarwal**[a,*]

[a]Departments of Pharmaceutical Sciences, Skaggs School of Pharmacy, University of Colorado Denver, Aurora, CO 80045, USA

[b]Department of Pathology, School of Medicine, University of Colorado Denver, Aurora, CO 80045, USA

[c]Department of Pediatrics, School of Medicine, University of Colorado Denver, Aurora, CO 80045, USA

Abstract

Sulfur mustard (SM) is a vesicant warfare agent which causes severe skin injuries. Currently, we lack effective antidotes against SM-induced skin injuries, in part due to lack of appropriate animal model(s) that can be used for efficacy studies in laboratory settings to identify effective therapies. Therefore, to develop a relevant mouse skin injury model, we examined the effects of nitrogen mustard (NM), a primary vesicant and a bifunctional alkylating agent that induces toxic effects comparable to SM. Specifically, we conducted histopathological and immunohistochemical evaluation of several applicable cutaneous pathological lesions following skin NM (3.2 mg) exposure for 12–120 h in SKH-1 and C57BL/6 mice. NM caused a significant increase in epidermal thickness, incidence of microvesication, cell proliferation, apoptotic cell death, inflammatory cells (neutrophils, macrophages and mast cells) and myleoperoxidase activity in the skin in both mouse strains. However, there was a more prominent NM-induced increase in epidermal thickness, and macrophages and mast cell infiltration, in SKH-1 mice relative to what was seen in C57BL/6 mice. NM also caused collagen degradation and edema at early time points (12–24 h); however, at later time points (72 and 120 h), dense collagen staining was observed, indicating either water loss or start of integument repair in both mouse strains. This study provides quantitative measurement of NM-induced histopathological and immunohistochemical cutaneous lesions in both hairless and haired mouse strains that could serve as useful tools for screening and identification of effective therapies for treatment of skin injuries due to NM and SM.

*Corresponding Author: Department of Pharmaceutical Sciences, Skaggs School of Pharmacy and Pharmaceutical Sciences, University of Colorado, 12850 E. Montview Blvd, Room V20-2118, Box C238, Aurora, CO 80045, USA. Tel: +303-724-4057; Fax: +303-724-7266; Rajesh.Agarwal@UCDenver.edu.
**Anil K. Jain and Neera Tewari-Singh equally contributed to this work

Conflict of Interest Statement
The authors declare that there are no conflicts of interest.

Keywords

Skin lesions; Inflammation; Microblisters; SKH-1 hairless mice; C57BL/6 mice; Nitrogen mustard

Introduction

Sulfur mustard [bis (2-chloroethyl) sulfide, SM], a vesicant, poses a potential threat of being used as a chemical warfare and terrorist weapon (Saladi et al., 2006, Sharma et al., 2010, Smith et al., 1995, Smith and Skelton, 2003). It is a bi-functional alkylating agent which causes severe skin injuries with delayed vesication, and has been used in World War I and II (Brookes and Lawley, 1961, Fidder et al., 1994, Shohrati et al., 2007). In humans, SM-caused skin injuries include erythema and edema, inflammation including dermal infiltration of inflammatory cells, blister formation and cell death of mainly basal epidermal keratinocytes with ulceration (Dacre and Goldman, 1996, Graham et al., 2005, Wormser, 1991). Currently, the absence of an appropriate animal model which can parallel skin lesions with SM exposure in humans has hindered the screening of agents in laboratory settings for the development of effective therapies against crippling skin injuries by this agent. There have been extensive research efforts to develop an appropriate animal model that parallels the human response to SM. Hence, clinical, histopathological, immunohistochemical and related mechanistic aspects of SM-induced skin lesions have been studied in several models including weanling pig, hairless guinea pig, hairless mouse, rabbit and bioengineered multilayered human skin (Greenberg et al., 2006, Hayden et al., 2009a). From the literature, it is evident that SM exposure causes pathological changes, vesication and inflammation in the skin of various animal models (Greenberg, Kamath, 2006, Shakarjian et al., 2010, Smith, Hurst, 1995, Smith et al., 1998); however, SM cannot be readily used in laboratory settings. With this in mind, our earlier studies have established inflammatory and vesication biomarkers in SKH-1 hairless mice using 2-chloroethyl ethyl sulfide (CEES), a SM analog (Jain et al., 2011b, Tewari-Singh et al., 2009). Although commonly used to study the effects of SM-induced skin toxicity, CEES is a mono-functional alkylating agent that is less toxic than SM (Jowsey et al., 2009, Tewari-Singh et al., 2010). Therefore, to more closely mimic the SM-induced gross pathology and other toxic effects, we conducted the current study using nitrogen mustard (NM), a bifunctional alkylating agent which alkylates DNA and induces DNA strand breaks which then leads to cell death in a manner similar to SM (Olsen et al., 1997, Osborne et al., 1995).

NM, an analog of SM, has not been directly used in warfare but is reported to have affected soldiers following a German attack that caused leakage from tankers in Italy. NM was stockpiled by several countries during World War II and still poses a similar threat to civilians and military personnel (Alexander, 1947, Papirmeister et al., 1985, Watson and Griffin, 1992). NM causes severe injuries primarily to the skin, eye and lung tissues, and is easy to synthesize, store, transport and use like SM (McManus and Huebner, 2005, Tewari-Singh et al., 2012b, Yaren et al., 2007). In addition, NM and SM at comparable doses cause parallel histopathological features and epidermal-dermal separation (Smith, Smith, 1998). Although there are a few reports describing skin lesions following NM exposure, most of these report were associated with evaluating the efficacy of the agents. A detailed study on the pathological effects of NM and the evaluation of these effects as biomarkers has not been reported (Anumolu et al., 2011, Gunhan et al., 2004, Milatovic et al., 2003, Wormser et al., 1997). Accordingly, here we conducted the histopathological and immunohistochemical evaluation of the skin pathologic lesions inflicted by NM in both SKH-1 hairless and C57BL/6 haired mouse strains. It is our optimism that the comparative presentation of the biomarkers of injury in SKH-1 hairless and C57BL/6 haired mice will help assess any statistically relevant differences in NM-related skin toxic effects and establish a relevant and

more useful laboratory skin injury model suitable for mechanistic and efficacy studies for NM- and SM-induced skin injuries.

Materials and Methods

Materials

NM (Mechlorethamine hydrochloride) was purchased from Sigma-Aldrich Chemicals Co. (St. Louis, MO). DeadEnd Colorimetric TUNEL System (Apoptosis detection kit) was purchased from Promega (Madison, WI), Ki67 and myeloperoxidase (MPO) antibody was purchased from Abcam (Cambridge, USA), and BM8 monoclonal F4/80 rat anti-mouse IgG2a antibody was obtained from Invitrogen, (Invitrogen, Carlsbad, CA) Gomori's trichrome stain and Weigert's Iron hematoxylin were purchased from Rowley Biochemical (MA, USA). MPO detection kit was purchased from Cell Technology (Mountain View, CA). Other chemicals used were purchased from Sigma-Aldrich Co. (St. Louis, MO) unless otherwise specified.

Animals

Male C57BL/6 and SKH-1 hairless mice (4–5 weeks of age) were purchased from Charles River Laboratories (Wilmington, MA) and housed under standard conditions at the University of Colorado Center of Laboratory Animal Care. Before starting the experiment with NM, the animals were acclimatized for one week according to the specified protocol approved by the IACUC of the University of Colorado Denver, CO. *Animal exposure to NM*. Prior to NM exposure, C57BL/6 mice were shaved and acclimatized and both mouse strains were exposed to NM (3.2 mg) based on the earlier studies as published (Tewari-Singh et al., 2013). NM was applied topically to the surface of the dorsal skin of the SKH-1 hairless and C57BL/6 mice in 200 ul acetone for 12 h, 24 h, 72 h and 120 h according to the previously published protocol. As reported earlier, acetone (200μl) alone was applied as a vehicle control on one group and another group of mice were kept without any exposure and used as an untreated control (Jain, Tewari-Singh, 2011b, Tewari-Singh, Rana, 2009, Tsai et al., 2001). Each study group consisted of 5 mice. Mice were euthanized following 12–120 of NM application and dorsal skin tissue was collected, fixed in 10% phosphate-buffered formalin for H&E staining, immunostaining and other histostaining processes. The remaining portion of the dorsal skin was frozen in liquid nitrogen for the MPO assay and molecular studies.

Hematoxylin and Eosin (H&E) staining and measurement of epidermal thickness and microvesication in skin sections

5μm skin tissue sections from both SKH-1 hairless and C57BL/6 mice were processed for H&E staining. Tissue sections from both mice strains were dehydrated in ethanol, cleared with xylene and embedded in paraffin (Triangle Biomedical Sciences, Durham, NC) as detailed earlier (Jain, Tewari-Singh, 2011b, Tewari-Singh, Rana, 2009). H&E stained slides of NM exposed skin samples from different time intervals were microscopically evaluated for epidermal thickness and microvesication. The epidermal thickness (μm) was measured randomly in at least five fields per tissue sample from two sets of H&E stained slides using Axiovision Rel 4.5 software (Carl Zeiss, Inc. Germany; 400× magnification). The incidence of microvesication was counted according to their sizes [1. small size (<100 μm^2) 2. medium size (100–500 μm^2) and 3. large size (>500 μm^2)] in 15–18 mm length of the skin sections. Histologically, microvesication was defined as separation of the epidermis from the dermis in which a spider web like accumulation of proteinaceous material was present.

Trichrome staining

Paraffin embedded skin tissue samples from both mouse strains were processed for trichrome staining by Gomori's one step trichrome method to analyze collagen I/III in NM exposed skin tissue. Skin samples were deparaffinized, hydrated and incubated in Bouin's solution for 1 h at 56°C. After washing in running water, sections were stained in Weigert's Iron hematoxylin for 10 min followed by staining with Gomori's trichrome stain with aniline blue for 20 min. After washing, the sections were dehydrated, cleared in xylene and mounted.

TUNEL staining to detect apoptotic cell death

Apoptotic cells death was analyzed in the control and NM exposed skin sections from both the mouse strains using the DeadEnd Colorimetric terminal deoxynucleotidyl transferase (tdt)-mediated dUTP-biotin nick end labeling (TUNEL) system according to the manufacturer's protocol as described earlier (Jain, Tewari-Singh, 2011b, Tewari-Singh, Rana, 2009). The brown colored TUNEL positive cells were quantified in 10 randomly selected fields at 400× magnification, and an apoptotic cell index was calculated as the number of apoptotic cells ×100 divided by total number of cells.

Immunohistochemical (IHC) staining for the detection of cell proliferation, macrophages and MPO

Paraffin embedded skin sections from both the mouse strains were deparaffinized, rehydrated, treated for antigen retrieval and immersed in 3% hydrogen peroxide to block the endogenous peroxide activity as reported earlier (Jain, Tewari-Singh, 2011b, Tewari-Singh, Rana, 2009). After washing, sections were incubated with mouse Ki67 antibody, BM8 monoclonal F4/80 rat anti-mouse IgG2a antibody or anti MPO antibody for the detection of cell proliferation, macrophages and MPO, respectively. The N-Universal negative control rabbit IgG antibody (DAKO) was used as a negative control. After washing, the sections were incubated with the appropriate biotinylated secondary antibody followed by incubation with HRP conjugated streptavidin (DAKO). The sections were washed in PBS and developed with DAB. Finally, sections were counterstained with Harris hematoxylin followed by dehydration and mounting for microscopic observation. The DAB positive nuclei were counted in 10 randomly selected fields (400× magnification), and the proliferation index was determined as number of Ki67 positive cells × 100 /total number of cells. The macrophages were counted per mm^2 field in five randomly selected fields per section (400 × magnification).

MPO activity

The MPO enzymatic activity in the control and NM exposed skin tissue of SKH-1 hairless and C57BL/6 mice was measured at 12 h, 24 h, 72 h and 120 h following exposure using a fluorescent MPO detection kit according to the manufacturer's protocol and as detailed in our previous publications (Jain, Tewari-Singh, 2011b, Tewari-Singh, Rana, 2009). In brief, 100 mg skin tissue samples from the mice were homogenized, 1 ml of solubilization buffer was added to the pellet and samples were further homogenized and the isolated protein estimated by Lowry's method. For MPO assay, 50 μl reaction mixture and 50 μl of prepared sample or serially diluted MPO (for the standard curve) were added in a 96-well opaque black plate for reaction. The plate was incubated in the dark for 60 min at RT and the fluorescence was measured at 530 nm excitation and 590 nm emissions. The blank reading was subtracted from the entire sample reading and the MPO activity was expressed as a mU/μg protein using the MPO standard curve.

Toluidine blue staining for mast cells

Toluidine blue staining for mast cells detection in the control and NM exposed skin sections of SKH-1 hairless and C57BL/6 mice was carried out according to the previously published protocol (Jain, Tewari-Singh, 2011b). Briefly, the sections were treated with toluidine blue working solution (5 ml toluidine blue + 45 ml of 1% sodium chloride) for 2–3 min, washed, dehydrated, cleared in xylene and mounted for microscopic observation. The mast cells were quantified by counting their number per mm^2 field in five randomly selected fields (×400 magnification).

Immunohistochemical and statistical analyses

The IHC analysis of the skin tissue sections was carried out using a Zeiss Axioscop 2 microscope (Carl Zeiss, Inc., Germany), and image analyses was done using Carl Zeiss Axiovision Rel 4.5 software. The data were analyzed and all statistical calculations were done using SigmaStat software version 2.03 (Jandal Scientific Corp., San Raphael, CA). Data are expressed as mean ± SEM and were analyzed via one way ANOVA followed by the Bonferroni t-test for multiple comparisons. $P< 0.05$ was considered statistically significant.

Results

NM exposure causes an increase in epidermal thickness and microvesication in both SKH-1 hairless and C57BL/6 mice

Earlier, we reported that exposure to NM caused clinical lesions including increased edema and microblister-like appearance in the skin of both haired and hairless mouse strains (Tewari-Singh, Jain, 2013). In the present study, first we quantified NM-induced epidermal thickness and incidence of microvesication in skin sections. In SKH-1 hairless mice, topical NM exposure for 12–120 h caused an increase in epidermal thickness, which was maximal (55.2μm) at 24 h after exposure in comparison with control (18.6 μm) mice (Fig. 1A and B). In C57BL/6 mice also, NM induced significant ($p<0.05$) increase in epidermal thickness, which was maximal (26.5 μm) at 72 h after exposure in comparison with control (15.9 μm) mice (Fig. 1C and D). These results showed that NM induced a more pronounced increase in epidermal thickness in SKH-1 hairless mice, reaching a maximum of 3 fold in comparison with the respective control at 24 h after exposure (Fig. 1B). Conversely, NM exposure caused a relatively smaller increase in epidermal thickness (1.6 fold) compared to control in C57BL/6 mice, where that change was maximal at 72 h after exposure (Fig. 1D).

Microvesication is one of the most significant markers of SM-induced skin injury in animal models; however, it causes vesication or blister formation in case of human skin (Shakarjian, Heck, 2010). Topical exposure of 3.2 mg NM resulted in the appearance of microvesication by 12 h, which became more prominent by 24 h after exposure in both SKH-1 and C57BL/6 mice (Tewari-Singh, Jain, 2013). These NM-induced microvesication lesions were next quantified according to lesion size [small size ($<100\mu m^2$), medium size ($100–500\mu m^2$) and large size ($>500\mu m^2$)]. In both SKH-1 hairless and C57BL/6 mice, NM induced microvesication of all sizes following 12–120 h of its exposure (Fig 1E–H). In SKH-1 hairless mice, large-sized microvesication lesions were maximal at 72 h and then decreased by 120 h (Fig. 1E and F); these lesions were also maximal at 72 h in C57BL/6 mice (Fig. 1G and H). No microvesication was observed in control skin tissue from either mouse strains.

NM exposure causes an increase in apoptotic cell death and cell proliferation in the epidermis of both SKH-1 hairless and C57BL/6 mice

Employing TUNEL staining, we next assessed apoptotic death in skin sections following NM exposure. Compared to control SKH-1 mice showing 23% apoptotic cell death, NM

exposure for 12, 24, 72 and 120 h resulted in 49%, 47%, 39% and 40% apoptotic cell death, respectively (Fig. 2A and B). Similarly, compared to 19% apoptotic cell death in control C57BL/6 mice, 34%, 38%, 25%, and 34% apoptotic cell death was observed following similar exposure times (Fig. 2C and D). Furthermore, NM exposure also caused an increased cell proliferation. This mitogenic response might in part be to compensate for apoptotic/necrotic cell death in the epidermis as identified by Ki67 staining (Fig. 2E–H), which is consistent with our previous study with CEES in SKH-1 hairless mice showing that cell proliferation is an important biomarker for SM-induced skin injury (Jain, Tewari-Singh, 2011b, Tewari-Singh, Rana, 2009). Compared to 23% cell proliferation in control SKH-1 hairless mouse skin, 35–46% proliferative cells were observed at 12–120 h after NM exposure (Fig 2E and F). Similar effects were also found in C57BL/6 mice with 39–44% proliferative cells after 12–120 h post-NM exposure versus only 26% such cells in control mice (Fig 2G and H).

NM exposure causes changes in collagen I/III levels in both SKH-1 hairless and C57BL/6 mice

A recent study has shown that SM affects collagen I/III network in mouse dermis (Joseph et al., 2011). To examine whether similar responses occur on collagen in the dermis following NM exposure, Gomori' trichrome staining was performed on NM-exposed skin tissue sections and the quantity/density of the royal blue stained collagen was graded as weak (+), strong (++) and very strong (+++). In SKH-1 hairless mice, weak trichrome staining was observed following 12–24 h of NM exposure where collagen fibers were disorganized accompanied by dermal thickening (Fig. 3A, Table 1). However, after 72 and 120 h after NM exposure, trichrome staining was strong with denser collagen fibers (Fig. 3A). Importantly, dermal thickness was maximal at 24 h after NM exposure and then decreased at 120 h after exposure to a thickness similar to control mice (Table 1). The same patterns of trichrome staining and dermal thickening were also seen in C57BL/6 mice after NM exposure; however, the intensity of collagen staining was more pronounced especially at 120 h after NM exposure as compared to SKH-1 hairless mice (Fig. 3B, Table 1).

NM exposure causes an increase in MPO activity indicating neutrophil infiltration, mast cells, and macrophages in both SKH-1 hairless and C57BL/6 mice

SM-caused inflammation and skin injury are reported in various animal models (Smith et al., 1997). MPO is an enzyme secreted by neutrophils with an important role in skin inflammation (Klebanoff, 2005), and thus we measured MPO activity in NM-exposed skin samples from both SKH-1 hairless and C57BL/6 mice. Following 12–120 h of NM exposure, a 13–18 and 9–10 fold increase in MPO activity was observed in SKH-1 hairless (Fig. 4A) and C57BL/6 mice (Fig. 4A), respectively. This observation was further supported IHC where positive staining within dermis intensified at epidermal-dermal junction at time points (72–120 h) following NM exposure in both SKH-1 and C57BL/6 mouse strains (Fig. 4B and C).

We next assessed the changes in mast cell numbers following NM exposure, as they could influence the recruitment of neutrophils at the injury sites (Eming et al., 2007). Toluidine blue-stained skin sections showed an NM-related increase in mast cell numbers that was more robust in SKH-1 hairless mice compared to C57BL/6 mice (Fig. 5A–D). Quantification of the mast cells in SKH-1 hairless mice revealed a significant ($p<0.001$) increase (cell density) after 12–72 h with maximal affect at 12–24 h after NM exposure with ~2 fold increase in mast cell number (Fig. 5B). Similar NM-caused responses were also observed in C57BL/6 mice with a significant ($p<0.001$) increase in mast cells (1.5 fold of controls) at 24 h after NM exposure (Fig. 5D).

Macrophages also play a pivotal role in the inflammation, hence these were assessed by IHC detection of F4/80 antigen in control and NM exposed skin samples of SKH-1 hairless and C57BL/6 mice (Fig. 5). A 2-fold increase in macrophage infiltration was observed at 12–24 h of NM exposure in SKH-1 hairless mice, which decreased at 72 and 120 h after exposure (Fig. 5E and F). In C57BL/6 mice, NM caused >5-fold increase in macrophage number at 12–24 h, which also decreased at 72 and 120 h after exposure (Fig. 5G and H).

Discussion

SM and NM are primary vesicating agents which cause severe skin tissue injury upon exposure in humans. Several studies have been done in animals to develop a relevant model for skin injury and efficacy studies for the development of novel therapeutics against SM-induced skin injury (Anumolu, Menjoge, 2011, Jain et al., 2011a, Pal et al., 2009, Shakarjian, Heck, 2010, Tewari-Singh et al., 2012a). However, SM models cannot be used routinely without containment facilities. Therefore, its analog NM has been used in the current study, which is a bi-functional alkylating agent with toxic effects similar to SM (Tewari-Singh, Jain, 2013). We employed both SKH-1 hairless and C57BL/6 haired mouse strains to establish quantifiable histopathological and immunohistochemical markers of NM-induced skin injuries.

As in our previous studies with SM analog CEES (Jain, Tewari-Singh, 2011b, Tewari-Singh, Rana, 2009), NM exposure showed that skin epidermal thickness could serve as an important marker of vesicant-related inflammation. Our results showed that NM exposure caused a more pronounced and significant epidermal thickening in SKH-1 hairless mice at all exposure time points (12–120 h) as compared to C57BL/6 mice, which could be indicative of a higher inflammatory response in SKH-1 hairless compared to C57BL/6 haired mice. Blister formation in humans and microblisters in animal models including mice, are the most significant lesions following SM exposure (Graham and Schoneboom, 2013, Greenberg, Kamath, 2006, Hayden et al., 2009b, Joseph, Gerecke, 2011, Poursaleh et al., 2012, Shakarjian et al., 2006, Shakarjian, Heck, 2010, Smith, Casillas, 1997). Histopathological assessment of NM-induced microblister like appearance on the skin of both SKH-1 and C57BL/6 mice showed epidermal-dermal separation at 12–120 h after its exposure. This study further supports earlier published reports where NM-exposure induced microvesication in mouse and human skin (Anumolu, Menjoge, 2011, Smith, Smith, 1998). Three sizes of microblisters from 100 to over 500 μm^2 were quantified for the first time here in both the mouse strains. In these studies, larger microvesicles were maximal in both the mouse strains at 72 h, which roughly parallels the small vesicle-like formation from 2–24 h following SM exposure in humans that later merge to form larger blister-like appearance by 48 h (Balali-Mood and Hefazi, 2005, Graham and Schoneboom, 2013).

A second significant lesion observed in SM-induced skin injury is apoptotic cell death of a portion of the basal keratinocytes (Mol et al., 2009, Tewari-Singh, Rana, 2009). NM-induced apoptotic cell death was observed between 12–120 h of NM exposure in both SKH-1 and C57BL/6 mice in this study. Our recent studies show that p53 plays an important role in NMinduced early apoptotic cell death (Inturi et al., 2013). Hence, this pathway and DNA damaging effect could play a significant role in NM-induced inflammation and skin injury similar to that reported for SM (Kehe et al., 2009, Kehe and Szinicz, 2005, Shakarjian, Heck, 2010). NMinduced apoptotic cell death observed here was also accompanied by an increase in Ki-67 staining indicating basal cell proliferation in both SKH-1 hairless and C57BL/6 mice. Ki-67 is a cell proliferation marker and this protein is present in nuclei of all active phases of the cell cycle except resting (G_0) phase (Scholzen and Gerdes, 2000). Therefore, our data suggests that damage in the basal keratinocytes initiates DNA damage repair and cell proliferation following apoptotic cell death by NM.

In skin, dermis contains a high content of thick collagen bundles. Recent studies in human skin explants have shown that NM or SM exposure does not cause any changes in collagens IV and VII (Smith, Smith, 1998). However, a compact collagen network was observed in the dermis following SM exposure in SKH-1 mouse skin. This network is hypothesized to be highly relevant to dermis remodeling after injury (Joseph, Gerecke, 2011). Our data showed an NM-induced thinning of collagen fibers accompanied by an increased dermal thickness at 12 and 24 h in both mouse strains. One interpretation of these results is that this could be due to edema and water retention following dermal injury. At later time points (72 and 120 h) after NM exposure, the collagen fibers appeared more compact and the collagen stained darker along with a decrease in dermal thickness. These changes appear to indicate the reformation of the dermal collagen lattice, an important step of wound healing in the skin. Alternatively, this could reflect excessive water loss from the skin of animals due to skin injuries, since at these time points following NM exposure, mice started losing weight and appeared to be dehydrated (Tewari-Singh, Jain, 2013).

SM skin injury is also associated with inflammatory cell infiltration into the dermis with an attendant release of inflammatory cytokines, which are thought to be important for the recruitment of a second round of inflammatory cells (Arroyo et al., 2001, Paromov et al., 2007, Sabourin et al., 2002, Wormser et al., 2005). In the present study, NM induced a robust increase in MPO activity indicating neutrophil infiltration in both mouse strains. Furthermore, NMinduced neutrophils were observed in the dermis as well as marginated in the vessels within the dermis showing an influx of these cells, which was consistent with previous reports using SM (Joseph, Gerecke, 2011, Wormser, Brodsky, 2005). The observed NM-induced MPO activity could serve as a valuable biomarker of vesicant skin injury based on the present study and earlier reports with SM and its analog CEES (Jain, Tewari-Singh, 2011b, Joseph, Gerecke, 2011, Tewari-Singh, Rana, 2009, Wormser, Brodsky, 2005). Our results also showed an NM-induced increase in macrophages in both mouse strains, with slightly higher number in SKH-1 hairless mice relative to C57BL/6 mice. The SM-induced increase in macrophages has been previously reported in animal models (Shakarjian, Heck, 2010, Tsuruta et al., 1996), and this too could serve as an important marker of vesicant skin exposure. In addition to an increase in neutrophils and macrophages, an increase in mast cells was also observed following NM exposure. Mast cell infiltration is associated with dermal neutrophils and macrophages (Joseph, Gerecke, 2011). After degranulation, mast cells secrete various inflammatory mediators like histamine, cytokines and various types of growth factors (Rao and Brown, 2008, Shiota et al., 2010). Significant mast cell infiltration in mouse skin after NM exposure is in agreement with our previous studies with CEES in SKH-1 hairless mice (Jain, Tewari-Singh, 2011b, Tewari-Singh, Rana, 2009). Since mast cell degranulation and infiltration are associated with SM-related skin injury in SKH-1 mice as seen with NM here (Joseph, Gerecke, 2011), this could be a more relevant skin injury model of vesicant injury.

In conclusion, this study reports for the first time the quantification of histopathological and immunohistochemical effects of NM-induced skin injury in both SKH-1 hairless and C57BL/6 mice. These quantified biomarkers and accelerated mouse skin injury model could be suitable for mechanistic and efficacy studies to screen therapeutics for NM- and SM-induced skin injuries.

Acknowledgments

This work was supported by the Countermeasures Against Chemical Threats (CounterACT) Program, Office of the Director National Institutes of Health (OD) and the National Institute of Environmental Health Sciences (NIEHS), [Grant Number U54 ES015678]. The study sponsor (NIH) had no involvement in the study design; collection, analysis and interpretation of data; the writing of the manuscript; and the decision to submit the manuscript for publications.

References

Alexander SF. Medical report on the Bari Harbor mustard casualties. Military surgeon. 1947; 101:1–17. [PubMed: 20248701]

Anumolu SS, Menjoge AR, Deshmukh M, Gerecke D, Stein S, Laskin J, et al. Doxycycline hydrogels with reversible disulfide crosslinks for dermal wound healing of mustard injuries. Biomaterials. 2011; 32:1204–1217. [PubMed: 20950853]

Arroyo CM, Broomfield CA, Hackley BE Jr. The role of interleukin-6 (IL-6) in human sulfur mustard (HD) toxicology. Int J Toxicol. 2001; 20:281–296. [PubMed: 11766126]

Balali-Mood M, Hefazi M. The pharmacology, toxicology, and medical treatment of sulphur mustard poisoning. Fundam Clin Pharmacol. 2005; 19:297–315. [PubMed: 15910653]

Brookes P, Lawley PD. The reaction of mono- and di-functional alkylating agents with nucleic acids. Biochem J. 1961; 80:496–503. [PubMed: 16748923]

Dacre JC, Goldman M. Toxicology and pharmacology of the chemical warfare agent sulfur mustard. Pharmacol Rev. 1996; 48:289–326. [PubMed: 8804107]

Eming SA, Krieg T, Davidson JM. Inflammation in wound repair: molecular and cellular mechanisms. The Journal of investigative dermatology. 2007; 127:514–525. [PubMed: 17299434]

Fidder A, Moes GW, Scheffer AG, van der Schans GP, Baan RA, de Jong LP, et al. Synthesis, characterization, and quantitation of the major adducts formed between sulfur mustard and DNA of calf thymus and human blood. Chemical research in toxicology. 1994; 7:199–204. [PubMed: 8199309]

Graham JS, Chilcott RP, Rice P, Milner SM, Hurst CG, Maliner BI. Wound healing of cutaneous sulfur mustard injuries: strategies for the development of improved therapies. J Burns Wounds. 2005; 4:e1. [PubMed: 16921406]

Graham JS, Schoneboom BA. Historical perspective on effects and treatment of sulfur mustard injuries. Chemico-biological interactions. 2013

Greenberg S, Kamath P, Petrali J, Hamilton T, Garfield J, Garlick JA. Characterization of the initial response of engineered human skin to sulfur mustard. Toxicological sciences : an official journal of the Society of Toxicology. 2006; 90:549–557. [PubMed: 16141436]

Gunhan O, Kurt B, Karayilanoglu T, Kenar L, Celasun B. Morphological and immunohistochemical changes on rat skin exposed to nitrogen mustard. Military medicine. 2004; 169:7–10. [PubMed: 14964494]

Hayden PJ, Petrali JP, Stolper G, Hamilton TA, Jackson GR Jr, Wertz PW, et al. Microvesicating effects of sulfur mustard on an in vitro human skin model. Toxicol In Vitro. 2009a; 23:1396–1405. [PubMed: 19619636]

Hayden PJ, Petrali JP, Stolper G, Hamilton TA, Jackson GR, Wertz PW, et al. Microvesicating Effects of Sulfur Mustard on an In Vitro Human Skin Model. Toxicology in vitro : an international journal published in association with BIBRA. 2009b

Inturi S, Tewari-Singh N, Jain AK, Roy S, White CW, Agarwal R. Absence of a p53 allele delays nitrogen mustard-induced early apoptosis and inflammation of murine skin. Toxicology. 2013; 311:184–190. [PubMed: 23845566]

Jain AK, Tewari-Singh N, Gu M, Inturi S, White CW, Agarwal R. Sulfur mustard analog, 2-chloroethyl ethyl sulfide-induced skin injury involves DNA damage and induction of inflammatory mediators, in part via oxidative stress, in SKH-1 hairless mouse skin. Toxicology letters. 2011a; 205:293–301. [PubMed: 21722719]

Jain AK, Tewari-Singh N, Orlicky DJ, White CW, Agarwal R. 2-Chloroethyl ethyl sulfide causes microvesication and inflammation-related histopathological changes in male hairless mouse skin. Toxicology. 2011b; 282:129–138. [PubMed: 21295104]

Joseph LB, Gerecke DR, Heck DE, Black AT, Sinko PJ, Cervelli JA, et al. Structural changes in the skin of hairless mice following exposure to sulfur mustard correlate with inflammation and DNA damage. Experimental and molecular pathology. 2011; 91:515–527. [PubMed: 21672537]

Jowsey PA, Williams FM, Blain PG. DNA damage, signalling and repair after exposure of cells to the sulphur mustard analogue 2-chloroethyl ethyl sulphide. Toxicology. 2009; 257:105–112. [PubMed: 19111594]

Kehe K, Balszuweit F, Steinritz D, Thiermann H. Molecular toxicology of sulfur mustard-induced cutaneous inflammation and blistering. Toxicology. 2009; 263:12–19. [PubMed: 19651324]

Kehe K, Szinicz L. Medical aspects of sulphur mustard poisoning. Toxicology. 2005; 214:198–209. [PubMed: 16084004]

Klebanoff SJ. Myeloperoxidase: friend and foe. J Leukoc Biol. 2005; 77:598–625. [PubMed: 15689384]

McManus J, Huebner K. Vesicants. Critical care clinics. 2005; 21:707–718. vi. [PubMed: 16168310]

Milatovic S, Nanney LB, Yu Y, White JR, Richmond A. Impaired healing of nitrogen mustard wounds in CXCR2 null mice. Wound repair and regeneration : official publication of the Wound Healing Society [and] the European Tissue Repair Society. 2003; 11:213–219.

Mol MA, van den Berg RM, Benschop HP. Involvement of caspases and transmembrane metalloproteases in sulphur mustard-induced microvesication in adult human skin in organ culture: directions for therapy. Toxicology. 2009; 258:39–46. [PubMed: 19167455]

Olsen LS, Korsholm B, Nexo BA, Wassermann K. Nitrogen mustard-mediated mutagenesis in human T-lymphocytes in vitro. Arch Toxicol. 1997; 71:198–201. [PubMed: 9049058]

Osborne MR, Wilman DE, Lawley PD. Alkylation of DNA by the nitrogen mustard bis(2-chloroethyl)methylamine. Chem Res Toxicol. 1995; 8:316–320. [PubMed: 7766817]

Pal A, Tewari-Singh N, Gu M, Agarwal C, Huang J, Day BJ, et al. Sulfur mustard analog induces oxidative stress and activates signaling cascades in the skin of SKH-1 hairless mice. Free radical biology & medicine. 2009; 47:1640–1651. [PubMed: 19761830]

Papirmeister B, Gross CL, Meier HL, Petrali JP, Johnson JB. Molecular basis for mustard-induced vesication. Fundamental and applied toxicology : official journal of the Society of Toxicology. 1985; 5:S134–S149. [PubMed: 2419197]

Paromov V, Suntres Z, Smith M, Stone WL. Sulfur mustard toxicity following dermal exposure: role of oxidative stress, and antioxidant therapy. Journal of burns and wounds. 2007; 7:e7. [PubMed: 18091984]

Poursaleh Z, Ghanei M, Babamahmoodi F, Izadi M, Harandi AA, Emadi SE, et al. Pathogenesis and treatment of skin lesions caused by sulfur mustard. Cutaneous and ocular toxicology. 2012; 31:241–249. [PubMed: 22122127]

Rao KN, Brown MA. Mast cells: multifaceted immune cells with diverse roles in health and disease. Ann N Y Acad Sci. 2008; 1143:83–104. [PubMed: 19076346]

Sabourin CL, Danne MM, Buxton KL, Casillas RP, Schlager JJ. Cytokine, chemokine, and matrix metalloproteinase response after sulfur mustard injury to weanling pig skin. Journal of biochemical and molecular toxicology. 2002; 16:263–272. [PubMed: 12481301]

Saladi RN, Smith E, Persaud AN. Mustard: a potential agent of chemical warfare and terrorism. Clinical and experimental dermatology. 2006; 31:1–5. [PubMed: 16309468]

Scholzen T, Gerdes J. The Ki-67 protein: from the known and the unknown. J Cell Physiol. 2000; 182:311–322. [PubMed: 10653597]

Shakarjian MP, Bhatt P, Gordon MK, Chang YC, Casbohm SL, Rudge TL, et al. Preferential expression of matrix metalloproteinase-9 in mouse skin after sulfur mustard exposure. Journal of applied toxicology : JAT. 2006; 26:239–246. [PubMed: 16489579]

Shakarjian MP, Heck DE, Gray JP, Sinko PJ, Gordon MK, Casillas RP, et al. Mechanisms mediating the vesicant actions of sulfur mustard after cutaneous exposure. Toxicological sciences : an official journal of the Society of Toxicology. 2010; 114:5–19. [PubMed: 19833738]

Sharma M, Vijayaraghavan R, Agrawal OP. Comparative toxic effect of nitrogen mustards (HN-1, HN-2, and HN-3) and sulfur mustard on hematological and biochemical variables and their protection by DRDE-07 and its analogues. International journal of toxicology. 2010; 29:391–401. [PubMed: 20466873]

Shiota N, Nishikori Y, Kakizoe E, Shimoura K, Niibayashi T, Shimbori C, et al. Pathophysiological role of skin mast cells in wound healing after scald injury: study with mast cell-deficient W/W(V) mice. Int Arch Allergy Immunol. 2010; 151:80–88. [PubMed: 19672099]

Shohrati M, Peyman M, Peyman A, Davoudi M, Ghanei M. Cutaneous and ocular late complications of sulfur mustard in Iranian veterans. Cutaneous and ocular toxicology. 2007; 26:73–81. [PubMed: 17612976]

Smith KJ, Casillas R, Graham J, Skelton HG, Stemler F, Hackley BE Jr. Histopathologic features seen with different animal models following cutaneous sulfur mustard exposure. J Dermatol Sci. 1997; 14:126–135. [PubMed: 9039976]

Smith KJ, Hurst CG, Moeller RB, Skelton HG, Sidell FR. Sulfur mustard: its continuing threat as a chemical warfare agent, the cutaneous lesions induced, progress in understanding its mechanism of action, its long-term health effects, and new developments for protection and therapy. J Am Acad Dermatol. 1995; 32:765–776. [PubMed: 7722023]

Smith KJ, Skelton H. Chemical warfare agents: their past and continuing threat and evolving therapies. Part I of II. Skinmed. 2003; 2:215–221. [PubMed: 14673274]

Smith KJ, Smith WJ, Hamilton T, Skelton HG, Graham JS, Okerberg C, et al. Histopathologic and immunohistochemical features in human skin after exposure to nitrogen and sulfur mustard. The American Journal of dermatopathology. 1998; 20:22–28. [PubMed: 9504665]

Tewari-Singh N, Gu M, Agarwal C, White CW, Agarwal R. Biological and molecular mechanisms of sulfur mustard analogue-induced toxicity in JB6 and HaCaT cells: possible role of ataxia telangiectasia-mutated/ataxia telangiectasia-Rad3-related cell cycle checkpoint pathway. Chemical research in toxicology. 2010; 23:1034–1044. [PubMed: 20469912]

Tewari-Singh N, Jain AK, Inturi S, Agarwal C, White CW, Agarwal R. Silibinin attenuates sulfur mustard analog-induced skin injury by targeting multiple pathways connecting oxidative stress and inflammation. PloS one. 2012a; 7:e46149. [PubMed: 23029417]

Tewari-Singh N, Jain AK, Inturi S, Ammar DA, Agarwal C, Tyagi P, et al. Silibinin, dexamethasone, and doxycycline as potential therapeutic agents for treating vesicant-inflicted ocular injuries. Toxicology and applied pharmacology. 2012b; 264:23–31. [PubMed: 22841772]

Tewari-Singh N, Jain AK, Inturi S, White CW, Agarwal R. Clinically-Relevant Cutaneous Lesions by Nitrogen Mustard: Useful Biomarkers of Vesicants Skin Injury in SKH-1 Hairless and C57BL/6 Mice. PloS one. 2013; 8:e67557. [PubMed: 23826320]

Tewari-Singh N, Rana S, Gu M, Pal A, Orlicky DJ, White CW, et al. Inflammatory biomarkers of sulfur mustard analog 2-chloroethyl ethyl sulfide-induced skin injury in SKH-1 hairless mice. Toxicological sciences : an official journal of the Society of Toxicology. 2009; 108:194–206. [PubMed: 19075041]

Tsai JC, Sheu HM, Hung PL, Cheng CL. Effect of barrier disruption by acetone treatment on the permeability of compounds with various lipophilicities: implications for the permeability of compromised skin. J Pharm Sci. 2001; 90:1242–1254. [PubMed: 11745777]

Tsuruta J, Sugisaki K, Dannenberg AM Jr, Yoshimura T, Abe Y, Mounts P. The cytokines NAP-1 (IL-8), MCP-1, IL-1 beta, and GRO in rabbit inflammatory skin lesions produced by the chemical irritant sulfur mustard. Inflammation. 1996; 20:293–318. [PubMed: 8796382]

Watson AP, Griffin GD. Toxicity of vesicant agents scheduled for destruction by the Chemical Stockpile Disposal Program. Environ Health Perspect. 1992; 98:259–280. [PubMed: 1486858]

Wormser U. Toxicology of mustard gas. Trends Pharmacol Sci. 1991; 12:164–167. [PubMed: 2063482]

Wormser U, Brodsky B, Green BS, Arad-Yellin R, Nyska A. Protective effect of povidone-iodine ointment against skin lesions induced by sulphur and nitrogen mustards and by non-mustard vesicants. Archives of toxicology. 1997; 71:165–170. [PubMed: 9049053]

Wormser U, Brodsky B, Proscura E, Foley JF, Jones T, Nyska A. Involvement of tumor necrosis factor-alpha in sulfur mustard-induced skin lesion; effect of topical iodine. Arch Toxicol. 2005; 79:660–670. [PubMed: 16001271]

Yaren H, Mollaoglu H, Kurt B, Korkmaz A, Oter S, Topal T, et al. Lung toxicity of nitrogen mustard may be mediated by nitric oxide and peroxynitrite in rats. Res Vet Sci. 2007; 83:116–122. [PubMed: 17196628]

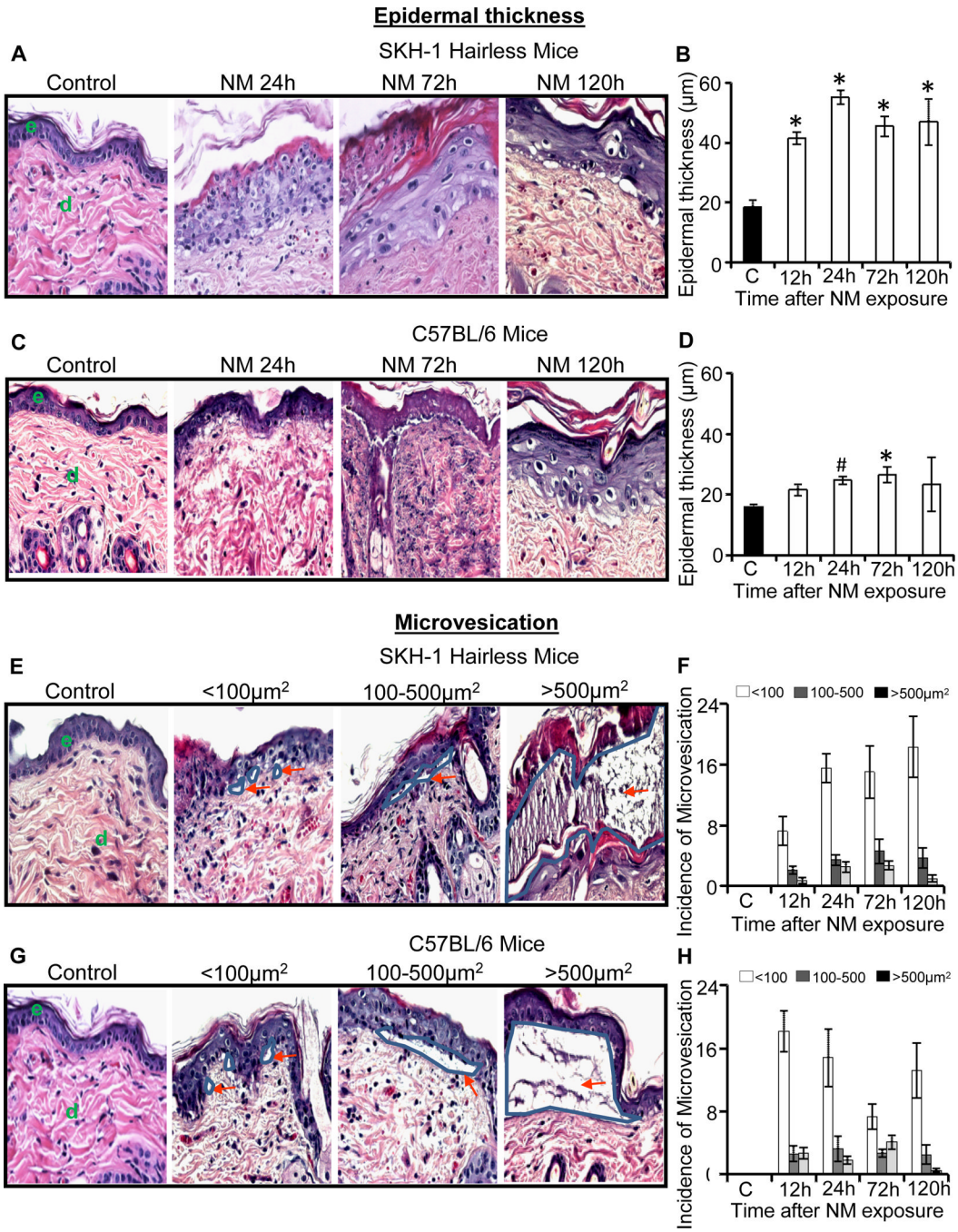

Fig. 1.

Topical application of NM on to the dorsal skin of SKH-1 hairless and C57BL/6 mice causes an increase in epidermal thickness and microvesication. Mice were exposed topically to either 200 μL of acetone alone or with NM (3.2 mg) in 200 μL acetone for 12–120 h and skin tissue was collected, processed, sectioned and subjected to H&E staining as detailed under materials and methods. The H&E stained skin tissue sections from both the mouse strains were analyzed for epidermal thickness (A–D) and microvesication (E–H). The NM-induced epidermal thickness in SKH-1 hairless and C57BL/6 mice is shown in representative pictures (A and C), and was further quantified (B and D) as detailed under materials and methods. NM-induced microvesication in SKH-1 hairless and C57BL/6 mice

is shown in representative pictures (E and G), which was further quantified according to their sizes (<100μm^2, 100–500 μm^2, >500 μm^2; F and H) as detailed under materials and methods. Data presented are mean ± SEM of three-five animals in each treatment group. Statistical significance of difference between NM and control groups were determined by one way ANOVA followed by Bonferroni t-test for pair wise multiple comparisons. *, $p<0.001$; $, $p<0.01$ and #, $p<0.05$ as compared to control. e, epidermis; d, dermis. Red arrows show the different sizes of microvesication.

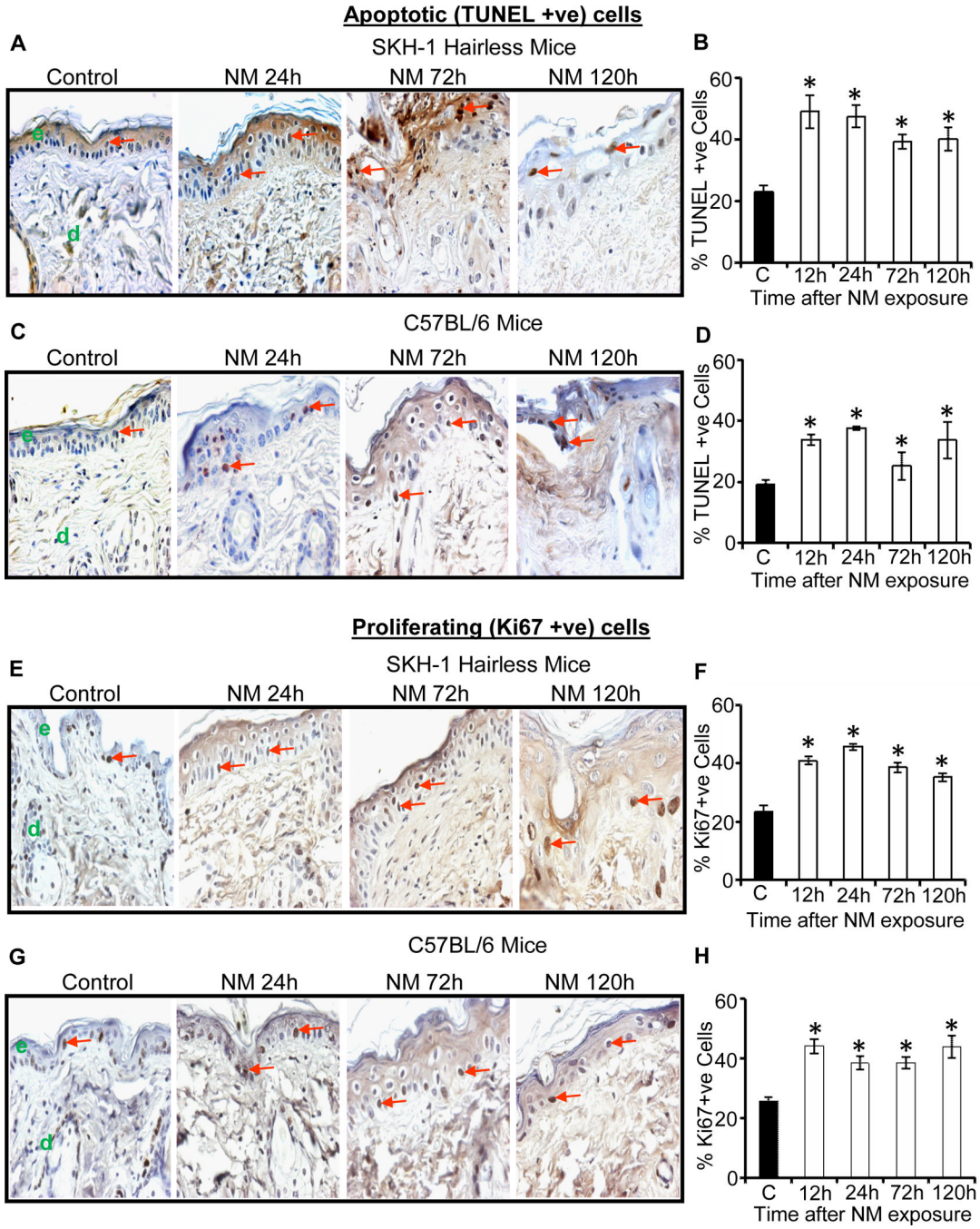

Fig. 2.

Topical application of NM causes an increase in apoptotic cell death and cell proliferation in male SKH-1 hairless and C57BL/6 mice skin. Mice were exposed topically to either 200 μL of acetone alone or with NM (3.2 mg) in 200 μL acetone for 12–120 h and skin tissue was collected, processed, sectioned and subjected to TUNEL staining (A–D) or Ki67 IHC (E–H) as detailed under materials and methods. NM-induced apoptotic cell death in TUNEL stained skin sections from SKH-1 hairless and C57BL/6 mice is shown in representative pictures (A and C), which was further quantified (B and D) as detailed under materials and methods. NM-induced cell proliferation in Ki67 IHC stained skin sections from SKH-1 hairless and C57BL/6 mice is shown in representative pictures (E and G), which was further

quantified (D and F) as detailed under materials and methods. Positive stained cells were counted per mm^2 field in randomly selected five fields per sample (×400 magnification). Data presented are mean ± SEM of three-five animals of each group. Statistical significance of difference between the NM exposed and control groups were determined by one way ANOVA followed by Bonferroni t-test for pair wise multiple comparisons. *, $p<0.001$ as compared to control group. e, epidermis; d, dermis; red arrows, TUNEL positive and Ki67 positive cells.

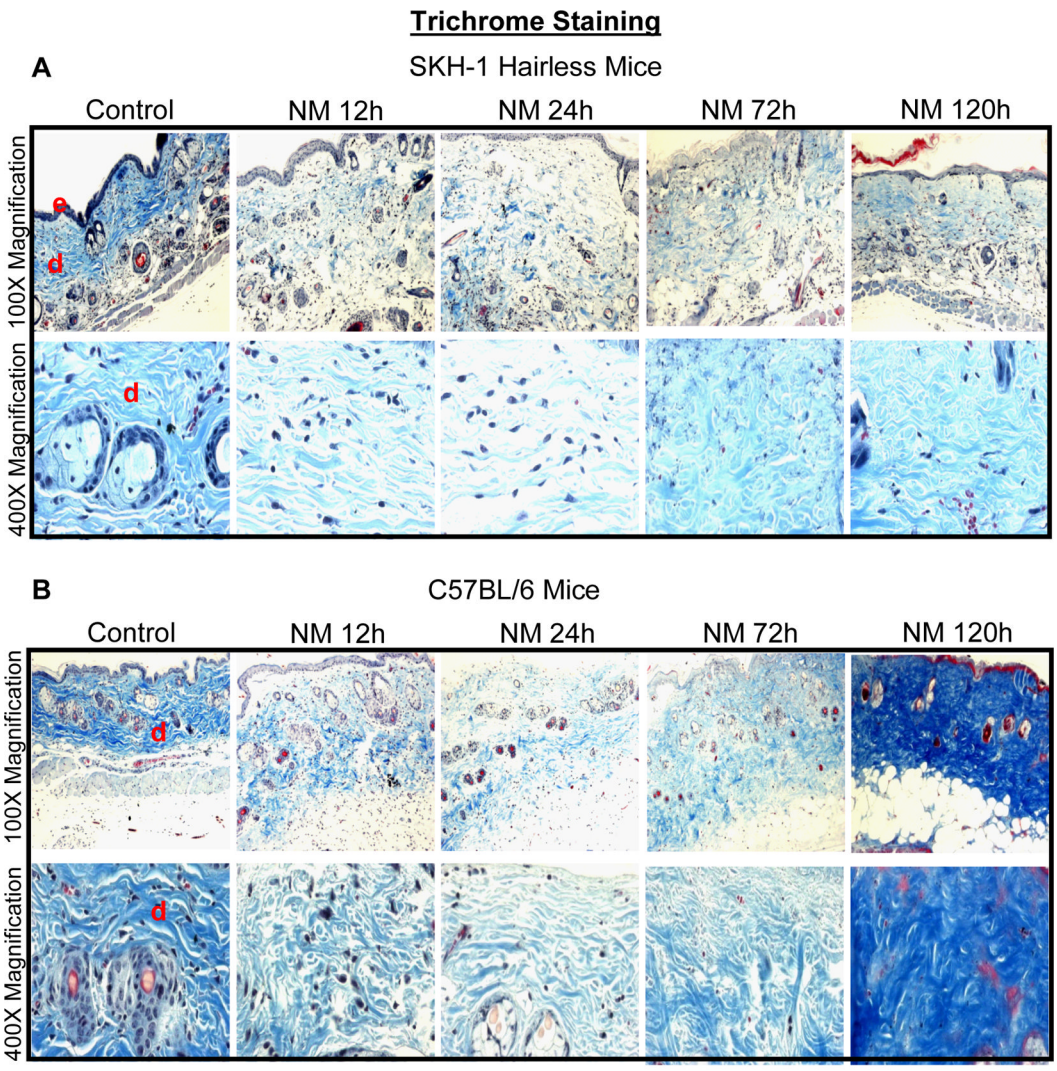

Table 1

		Control	NM12h	NM 24h	NM 72h	NM120h
SKH-1	Grading	++	+	+	++	++
	Thickness (μm)	329.3±9	364±12	396±19	372.3±21	323.3±24
C57BL6/J	Grading	+++	++	+	++	+++
	Thickness (μm)	393.3±38	446±8	453.3±18	440.8±27	402.2±13

Fig. 3.

Topical application of NM causes changes in dermal collagen staining and thickness in SKH-1 hairless and C57BL/6 mice skin. Mice were exposed topically to either 200 μL of acetone alone or with NM (3.2 mg) in 200 μL acetone for 12–120 h and skin tissue was collected, processed, sectioned and subjected to Gomori's trichrome staining. NM-induced changes in collagen staining and organization, and dermal thickness in Gomori's trichrome stained skin sections from SKH-1 hairless and C57BL/6 mice is shown in representative pictures (A and C), staining was further graded (+, weak staining; ++ strong staining; +++, very strong staining) and dermal thickness quantified (Table 1) as detailed under materials and methods. Collagen stained royal blue and nuclei stained dark blue/black. Grading and

thickness were observed in three-five animals at each time point after NM exposure. e, epidermis; d, dermis

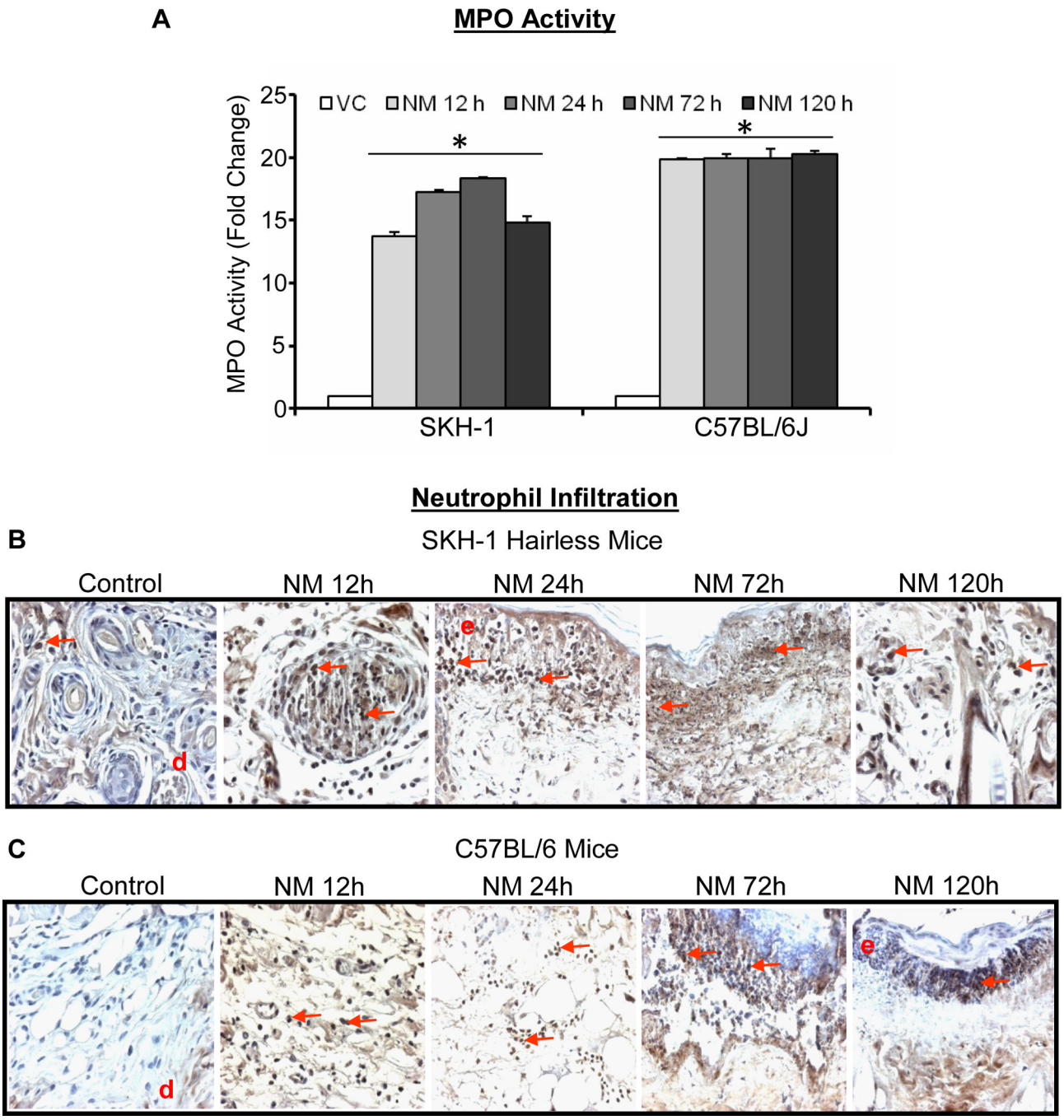

Fig. 4.

Topical application of NM causes an increase in MPO activity and neutrophil infiltration in skin of SKH-1 hairless and C57BL/6 mice skin. Mice were exposed topically to either 200 μL of acetone alone or with NM (3.2 mg) in 200 μL acetone for 12–120 h and skin tissue was collected and frozen. MPO activity was determined in the skin samples using MPO fluorescence assay kit as detailed under materials and methods (A). Skin from exposed mice was also collected, processed, sectioned and subjected to MPO IHC as detailed under material and methods (B and C). NM-induced MPO activity in MPO IHC stained skin sections from SKH-1 hairless and C57BL/6 mice is shown in representative pictures (B and C), Data presented are mean ± SEM of three-five animals in each treatment group and

samples were taken in duplicate for the MPO assay. Statistical significance of difference between the NM exposed and control groups were determined by one way ANOVA followed by Bonferroni t-test for pair wise multiple comparisons. *, $p<0.001$ as compared to control group. d, dermis; red arrows, MPO positive cells.

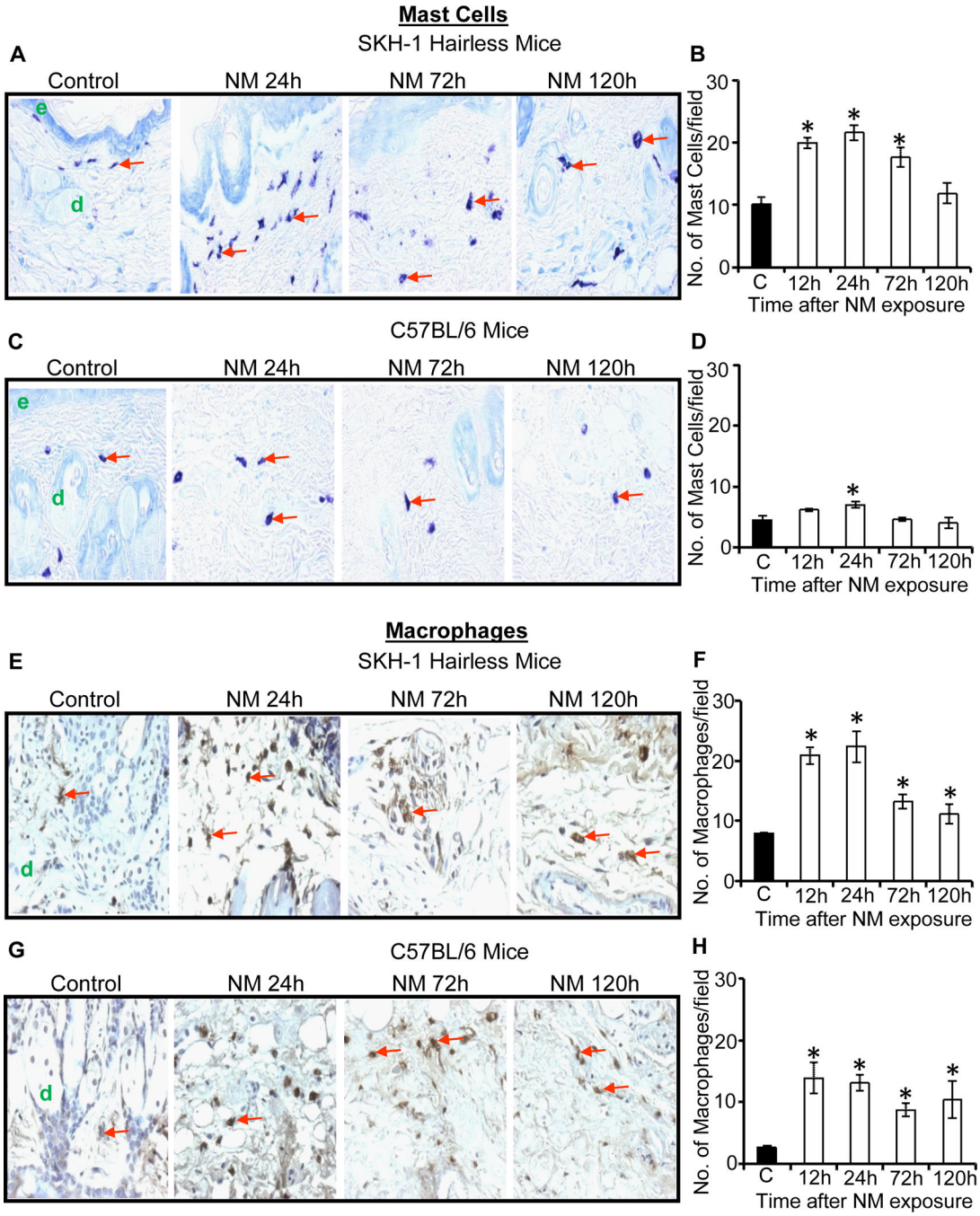

Fig. 5.

Topical application of NM causes an increase in the number of mast cells and macrophages in the skin of male SKH-1 hairless and C57BL/6 mice. Mice were exposed topically to either 200 μL of acetone alone or with NM (3.2 mg) in 200 μL acetone for 12–120 h and skin tissue was collected, processed, sectioned and subjected to toluidine blue staining (A–D) or F4/80 IHC (E–H) as detailed under materials and methods. NM-induced increase in mast cell numbers in toluidine blue stained skin sections from SKH-1 hairless and C57BL/6 mice is shown in representative pictures (A and C), which was further quantified (B and D) as detailed under materials and methods. NM-induced increase in macrophages in F4/80 IHC stained skin sections from SKH-1 hairless and C57BL/6 mice is shown in

representative pictures (E and G), which was further quantified (F and H) as detailed under materials and methods. Positive stained cells (mast cells and macrophages) were counted per mm^2 field in randomly selected five fields per sample (×400 magnification) as detailed in materials and methods. Data presented are mean ± SEM of three-five animals of each group. Statistical significance of difference between the NM exposed and control groups were determined by one way ANOVA followed by Bonferroni t-test for pair wise multiple comparisons. *, $p<0.001$ compared to control group. e, epidermis; d, dermis; red arrows, mast cells and macrophages.

Table 1

Grading of Collagen I/III by Gomori's trichrome staining and dermal thickness in NM-exposed skin of SKH-1 hairless and C57BL/6 mice.

Mice	Score	Control	NM 12 h	NM 24 h	NM 72 h	NM 120 h
SKH-1	Grading	++	+	+	++	++
	Thickness (μm)	329.3±9	364.0±12	396.0±19	372.3±21	323.3±24
C57BL/6	Grading	+++	++	+	++	+++
	Thickness (μm)	393.3±38	446.0±8	453.3±18	440.8±27	402.2±13

+, weak staining; ++ strong staining; +++, very strong staining